

An impedance immunosensor for the detection of the phytohormone abscisic acid

Yu-Wei Li · Kai Xia · Ruo-Zhong Wang ·
Jian-Hui Jiang · Lang-Tao Xiao

Received: 31 March 2008 / Revised: 24 May 2008 / Accepted: 28 May 2008 / Published online: 16 June 2008
© Springer-Verlag 2008

Abstract The phytohormone abscisic acid (ABA) is the major player in mediating the adaptation of plants to stress. Previously developed phytohormonal biosensors usually employed indirect detection of the products of conjugated oxidase reactions. A label-free electrochemical impedance immunosensor for ABA detection was developed using an anti-ABA antibody adsorbed directly on a porous nanogold film. The film was produced electrochemically on a glassy carbon electrode in 0.008 mol/L hydrogen tetrachloroaurate solution containing 0.004 mol/L lead acetate with an applied potential of -0.5 V (versus Ag/AgCl) for 50 s. The anti-ABA antibody was immobilized onto the porous nanogold through electrostatic adsorption and covalent conjugation. Electrochemical impedance spectroscopy was used to characterize the successful construction of the porous nanogold film and the stepwise modification of the glassy carbon electrode. The concentration increase of the antigen brought about a decrease of the interfacial electron transfer, which also meant an increase of the impedance signal. The experimental parameters pH, antibody incubation time, and antibody concentration were optimized. The results showed significant linearity $R=0.9942$, with the content of ABA in the range 0.5–5,000 ng/mL with a detection limit at about 0.1 ng/mL.

Keywords Impedance immunosensor ·
Abscisic acid · Immunoassay · Porous nanogold

Introduction

Abscisic acid (ABA), the stress phytohormone in higher plants, regulates several important physiological functions, including response to abiotic stress (abnormal temperature, ultraviolet, drought, etc.), regulation of seed dormancy and germination, and control of stomatal movement [1, 2]. The content of a phytohormone in a plant is usually low, for instance, the tissue concentration for phytohormones usually ranges from 10 to 100 ng/g for indole-3-acetic acid, from 1 to 100 ng/g for gibberellins, from 1 to 100 ng/g for cytokinins, and from 10 to 50 ng/g for ABA. In addition, phytohormones are easily decomposed by heat, light, and oxygen. Hence, plant physiologists urgently require a rapid, precise, and convenient measurement procedure for phytohormonal assay in plants. Traditional phytohormonal analysis techniques such as gas chromatography [3, 4], gas chromatography/mass spectrometry [5], liquid chromatography/mass spectrometry [6], capillary electrophoresis [7], high-performance liquid chromatography (HPLC) [8, 9], enzyme-linked immunosorbent assay [10], and radioimmunoassay [11] have been broadly reported. However, the requirement of sophisticated instrumentation and radioactive chemicals and the time-consuming nature of traditional assays have created the need for a simple, accurate, and fast method for phytohormonal assay. This paper reports the development of an impedance immunosensor on the basis of anti-ABA antibody adsorbed directly on a porous nanostructured gold film to determine ABA.

Nanoparticles, in particular gold nanoparticles, have been successfully applied to electrochemical immunoassay of DNA because of its intrinsic strong adsorption property and biocompatibility. Presently, gold nanoparticles are used

Y.-W. Li · R.-Z. Wang · L.-T. Xiao (✉)
Hunan Provincial Key Laboratory of Phytohormones and Growth
Development, Hunan Agricultural University,
Furong District,
Changsha Hunan 410128, China
e-mail: langtaoxiao@163.com

K. Xia
College of Agronomy, Nanjing Agricultural University,
Nanjing 210095, China

J.-H. Jiang
State Key Laboratory of Chemo/Biosensing and Chemometrics,
Hunan University,
Changsha 410082, China

to label biochemicals or as matrix material to immobilize biochemicals. Tedious procedures were required to assemble gold nanoparticles onto an electrode surface [12, 13]. Electrochemical deposition of gold nanoparticles is a promising method to form a three-dimensional nanostructured film on electrodes, which allows for a higher degree of immobilization of bioreceptor molecules per unit area, presumably resulting in a stronger biosensor signal [14], and has been used to adsorb surface-layer protein.

Several immunosensors have been developed to detect phytohormones, and important results were obtained [15–17]. However, these immunosensors employ indirect detection of the products of horseradish peroxidase [16] or need the phytohormone molecules to conjugate with bovine serum albumin (BSA) [17]. In the work reported here, we employed a new immunoassay to detect ABA, based on depositing a porous nanostructured gold film on a glassy carbon electrode, and adsorbing the anti-ABA antibody directly on the gold film.

Materials and methods

Apparatus and reagents

ABA and hydrogen tetrachloroaurate hydrate were purchased from Sigma-Aldrich, lead acetate was received from Harbin Chemical Reagent Co. (Heilongjiang, China), BSA was obtained from Beijing Dingguo Biotechnology Development Center (Beijing, China), and monoclonal anti-ABA antibody was provided by Nanjing Agricultural University with a titer of 1:1,000 [18]. Other reagents were of analytical reagent grade. Double-distilled water was used throughout.

The impedance measurements were performed at room temperature using with a conventional three-electrode system, with a modified glassy carbon electrode serving as the working electrode, platinum foil as the counter electrode, and a saturated calomel electrode as the reference electrode, using a CHI760C electrochemical workstation from Shanghai Chenhua Instrument Co. (Shanghai, China) linked to a personal computer. Impedance spectra were recorded over a frequency range from 0.01 to 100,000 Hz with an alternating current potential amplitude of ± 5 mV, starting with an initial potential of 0.235 V. HPLC analysis was performed with an Agilent 1100 instrument, while scanning electron microscopy (SEM) was carried out using a JSM-6380(LV) system.

Preparation of the modified electrode and fabrication of the immunosensor

A glassy carbon electrode (4 mm diameter) was carefully polished with polishing paper and 1.0-, 0.3-, and 0.05- μm

alumina slurry on a woolen cloth, and then thoroughly cleaned with water, ethanol, and fresh piranha solution (1:3 30% H_2O_2 and concentrated H_2SO_4). Then, the electrochemical deposition of a porous nanostructured gold film was performed in a 5-mL cell of 0.08 mol/L hydrogen tetrachloroaurate solution containing 0.004 mol/L lead acetate. The porous nanostructured gold film grew on the glassy carbon electrode under an applied potential of -0.5 V (Ag/AgCl) for 50 s. Then, the modified glassy carbon electrode was washed thoroughly with distilled water and dried with nitrogen before being incubated in anti-ABA antibody solution (pH 7.4) at a titer of 1:1,000 for 1 h at room temperature. After the electrode had been washed with water, 16 μL of 1.0 mg/mL BSA of pH 7.4 was dropped onto the modified electrode surface for 30 min at room temperature to block the remaining free binding sites to prevent unspecific binding to the sensor. A 16- μL aliquot of 0.2 mg/mL ABA standard solution was dropped on the immunosensor surface subsequently after washing the electrode with water, and incubation for 1 h at 37 $^\circ\text{C}$ yielded the antibody-antigen complex on the immunosensor. For the steady-state experiment, the impedance of the biosensor interface was measured periodically until the steady state was reached.

Immunoassay procedure

A three-electrode system with the immunosensor as the working electrode was used in a thermostated cell at 36.0 ± 0.3 $^\circ\text{C}$ with 5 mL phosphate-buffered saline (pH 7.4) containing 0.1 mol/L KCl and 0.01 mol/L $\text{K}_3[\text{Fe}(\text{CN})_6]/\text{K}_4[\text{Fe}(\text{CN})_6]$. The impedance spectra of the immunosensor were taken (1) after the incubation of anti-ABA antibody and blocking with BSA and (2) after the immersion into the ABA solution. The impedances were recorded as Z_0 and Z_1 , respectively. The percentage of impedance enhancement is given by Eq. 1:

$$(\Delta Z/Z_0)\% = \frac{Z_1 - Z_0}{Z_0} \times 100. \quad (1)$$

A series of standards of ABA were used to construct the calibration curve, which could be used for the determination of ABA in unknown samples.

Preparation of plant material samples

Fresh samples from hybrid rice were frozen in liquid nitrogen and immediately lyophilized for 48 h. To prevent light exposure, the samples were kept in the dark throughout the process. Each sample (1.0 g) was ground in a porcelain mill, passed through a 40-mesh screen, then collected in a vessel and mixed with 15 mL of 80% (v/v) methanol for overnight extraction in a refrigerator. The

supernatant was collected after centrifugation at 15,000 rpm for 20 min, and purified via a poly(vinylpyrrolidone)-(diethylamino)ethyl column system and collected in Waters C18 Sep-Pak cartridges. A 5-mL aliquot of 50% (v/v) methanol was used to elute ABA from the Sep-Pak cartridges, and the ABA was dried in a Jouan vacuum concentration system. Finally the samples were dissolved in 200 μL of distilled water for the following assay.

Results and discussion

Surface characterization by SEM

The resulting gold surface was characterized using SEM as shown in Fig. 1. Anomalous porous clusters were obtained on the glassy carbon electrode. The sizes of the clusters varied from 15 to 30 μm , which was probably caused by different deposition times. Apparently, the porous nanogold film formed after electrochemical deposition greatly enlarged the surface of the bare carbon electrode.

Characterization of the immunosensor

The application of electrochemical impedance methods to probing biomolecular interactions at surfaces has been reported [19–21]. In most impedance biosensor studies, a redox probe such as $[\text{Fe}(\text{CN})_6]^{3-/4-}$ is added to the analyte to decrease the measured impedance value. Otherwise, the alternating current response becomes quite small, which may decrease the experimental sensitivity. In a Nyquist representation, the real component, Z' , of the complex impedance is shown on the abscissa, and the imaginary component, Z'' , on the ordinate. The two components

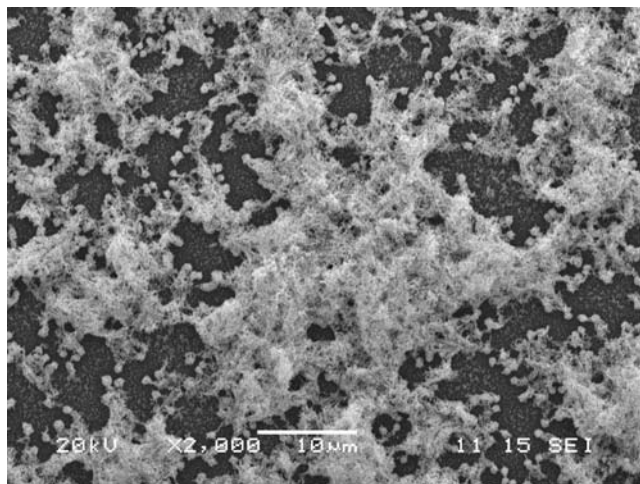


Fig. 1 A scanning electron microscopy photograph of a porous nanogold film modified glassy carbon electrode surface

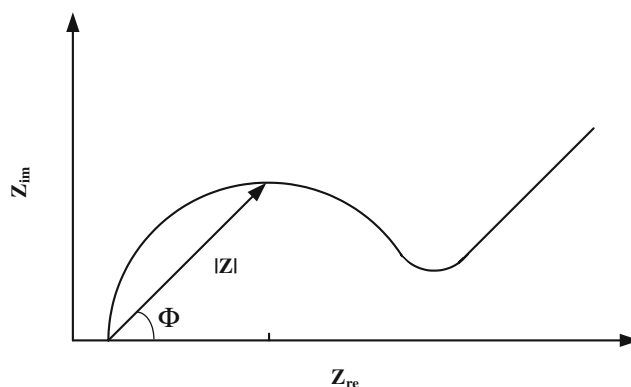


Fig. 2 A typical Nyquist plot (Z_{im} vs. Z_{re}) of a faradic impedance spectrum

originating, respectively, from the resistance and the capacitance of the cell sum up as the complex impedance, which is

$$Z = Z' + iZ'' \quad (2)$$

The magnitude of the impedance, $|Z|$, can be expressed as follows:

$$|Z| = \left(Z'^2 + Z''^2 \right)^{1/2} \quad \text{and} \quad \tan \phi = Z''/Z'. \quad (3)$$

In Fig. 2, a semicircle and a straight line with a slope of 45° appear at higher and lower frequencies. The semicircle portion corresponds to the electron-transfer-limited process, and the linear portion represents the diffusion-limited process. The diameter of the semicircle corresponds to the charge-transfer resistance, R_{ct} , which is inversely related to the charge-transfer rate at the electrode interface. Its values

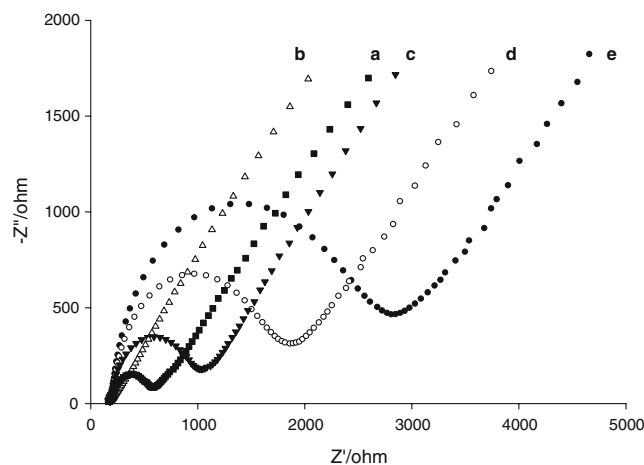


Fig. 3 Nyquist plots (Z_{im} vs. Z_{re}) for faradic impedance measurements in the presence of 0.01 mol/L $\text{K}_3[\text{Fe}(\text{CN})_6]/\text{K}_4[\text{Fe}(\text{CN})_6]$ corresponding to *a* glassy carbon electrode, *b* porous nanostructured gold film modified glassy carbon electrode, *c* incubation with 0.5 $\mu\text{g}/\text{mL}$ anti-absicic acid (anti-ABA) antibody solution, *d* blocking with bovine serum albumin solution, and *e* further incubation with ABA solution

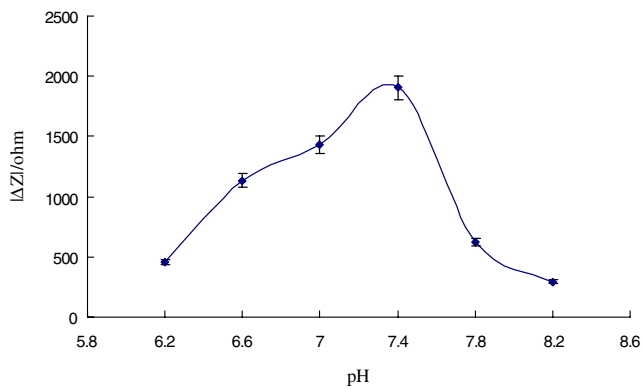


Fig. 4 Effect of pH of the incubation solution on antibody adsorption (means \pm s, $n=5$)

vary when different substances are adsorbed onto the electrode surface.

The impedance features are presented as Nyquist plots for the electrodes at different modification steps (Fig. 3). Significant differences (99% confidence interval) in the impedance spectra were observed during stepwise formation of the multilayer films on the electrode. For a bare glassy carbon electrode, curve a in Fig. 3 consists of a small semicircle probably due to the resistance of the thin oxidative layer. The impedance of the electrode after the deposition of the nanogold is given by a straight line (Fig. 3, curve b), implying that the electron-transfer process is not a limiting step of the electrochemical process. The adsorption of anti-ABA antibody is represented by a semicircle lying on the x -axis (Fig. 3, curve c), indicating a higher electron-transfer resistance at the electrode interface. After the adsorption of BSA and ABA, the diameters of the semicircle parts increased accordingly. This indicates the interfacial charge rate of $\text{Fe}(\text{CN})_6^{4-}/\text{Fe}(\text{CN})_6^{3-}$ is decreased, corresponding to the increase in diameters. It is attributed to the hindrance effect to the redox couples, which originates from the insulating protein

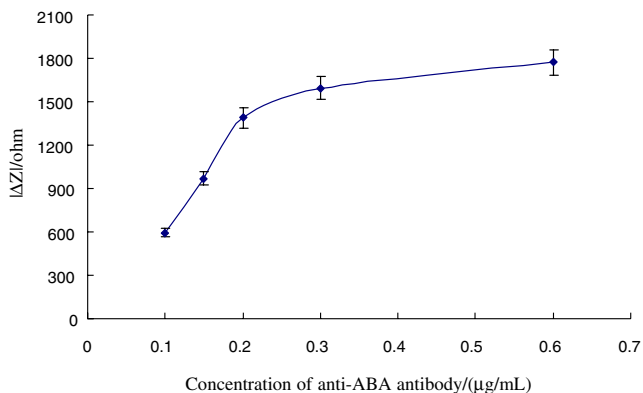


Fig. 5 Change in the magnitude of the impedance for different concentrations of anti-ABA antibody (means \pm s, $n=5$)

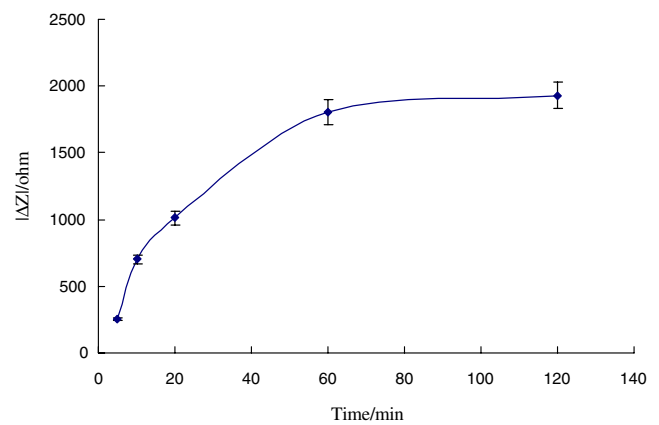


Fig. 6 Effect of adsorption time on the change in the magnitude of the impedance (means \pm s, $n=5$)

adsorbed on the electrode. Upon the stepwise formation of the insulating films, the electrical contact between $\text{Fe}(\text{CN})_6^{4-}/\text{Fe}(\text{CN})_6^{3-}$ and the electrode surface was inhibited.

Optimization of the assay conditions

The operating pH, temperature, absorption time, and concentration of anti-ABA antibody were investigated to optimize analytical performance. The anti-ABA antibody on the electrode generates a barrier for electron transfer. Generally, the more antibody that was adsorbed, the bigger the impedance change would be.

The effect of pH on the adsorption of the antibody onto the porous nanostructured gold film was evaluated over a pH range from 6.2 to 8.2. The gold-modified glassy carbon electrode was coated with 16 μL of anti-ABA antibody solution at different pH values for 1 h. The impedance was recorded by faradic impedance measurement. As shown in Fig. 4, the impedance reached the highest value at pH 7.4,

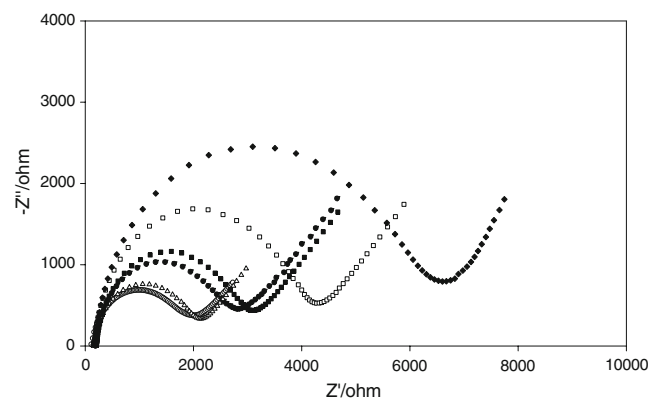


Fig. 7 Nyquist plots (Z_{im} vs. Z_{re}) for faradic impedance measurements in the presence of 0.01 mol/L $\text{K}_3[\text{Fe}(\text{CN})_6]/\text{K}_4[\text{Fe}(\text{CN})_6]$ for the immunosensor after incubation with different concentrations of ABA from 0.5 to 5,000 ng/mL under the optimal experimental conditions

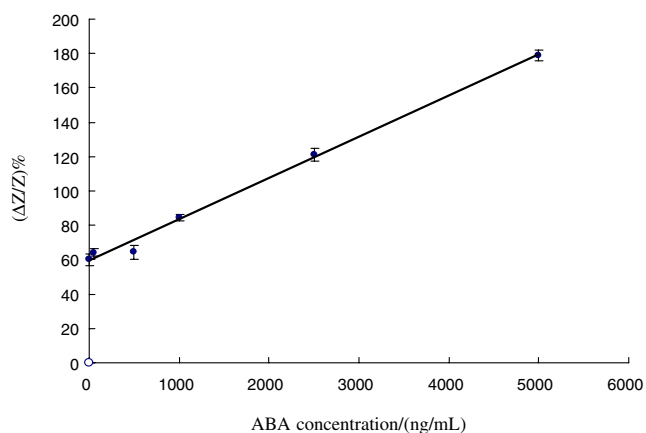


Fig. 8 Calibration curve for ABA. The vertical bars designate the standard deviation for the mean of five repeat tests

indicating the maximal adsorption was obtained at this value. The optimum pH of 7.4 was therefore used for adsorption of anti-ABA antibody onto gold-film-modified glassy carbon electrodes.

The concentration of anti-ABA antibody incubated onto the electrode determines the amount of ABA bound to the immunosensor surface to bring about the impedance response. As shown in Fig. 5, the increase of the anti-ABA antibody concentration seems to be beneficial for obtaining an increased impedance response. When the concentration of the antibody is higher than 0.3 $\mu\text{g/mL}$, the impedance response becomes sluggish, which might be attributed to the interaction between the macromolecules and the limitation of the active binding sites for protein. Thus, in the experiment, an antibody concentration of 0.5 $\mu\text{g/mL}$ was used.

The dependency of the impedance shift on the incubation time during the immobilization of anti-ABA antibody on the porous gold surface is shown in Fig. 6. The gold-film-modified glassy carbon electrodes were coated with 16 μL of 0.5 $\mu\text{g/mL}$ antibody solution of pH 7.4 for different times. The results show that an incubation time shorter than 60 min seems to be insufficient for anti-ABA antibody immobilization with sufficient coverage of the sensor surface. The impedance becomes stable after 60 min; thus, an adsorption time of 60 min was selected.

Table 1 Determination of abscisic acid (ABA) in *Oryza sativa* leaf samples by high-performance liquid chromatography (HPLC) and the ABA impedance immunosensor (means \pm s, $n=3$)

Sample no.	HPLC (ng/g)	Immunosensor (ng/g)
1	141.2 \pm 3.7	131.8 \pm 14.6
2	170.1 \pm 4.4	159.3 \pm 16.5
3	158.9 \pm 3.9	146.1 \pm 16.6

Calibration and the analysis of plant samples

Figure 7 shows the response of the current impedance biosensor as a function of ABA concentration, choosing as the response the change in the impedance magnitude, illustrating that a linear response can be obtained within the range from 0.5 to 5,000 ng/mL. The linear equation was $y = 0.0239x + 59.615$, with a statistically significant correlation coefficient of 0.9942 (Fig. 8). The detection limit of this label-free impedance detection assay was about 0.1 ng/mL. The results of the analysis of three samples are presented in Table 1, and showed the feasibility of using the proposed method for the analysis of plant samples.

Conclusions

An immunosensor based on the deposition of porous nanostructured gold film on a glassy carbon electrode was described, providing a general electrochemical impedance method for the label-free direct detection of ABA in plant samples. In addition, an important advantage of impedance-based biosensors is that they are not restricted to redox enzymes for signal detection.

Acknowledgements This work was supported by the National Natural Science Foundation of China (grants nos. 30670190 and 30600049), Hunan Provincial Science and Technology Key Project (grants nos. 2007FJ2003 and 2006NK1001), and the National Commonweal Research Project of China for Quality Supervision, Inspection and Quarantine (grant no. 2007GYB146).

References

- Davies PJ (2004) (ed) The plant hormones: biosynthesis, signal transduction, action. Kluwer, Dordrecht
- Nambara E, Marion-Poll A (2005) Annu Rev Plant Biol 56:165–185
- Hedden P (1993) Annu Rev Plant Physiol 44:107
- Birkemeyer C, Kolasa A, Kopka J (2003) J Chromatogr A 993(1–2):89–102
- Perrine FM, Rolfe BG, Hynes MF, Hocart CH (2004) Plant Physiol Biochem 42(9):723–729
- Carbonell ML, Jáuregui O (2005) Plant Physiol Biochem 43(4):407–411
- Olsson J, Claeson K, Karlberg B, Nordstrom AC (1998) J Chromatogr A 824:231–239
- López-Carbonell M, Jáuregui O (2006) Plant Physiol Biochem 43(4):407–411
- Dobrev PI, Havlicek L, Vagner M, Malbeck J, Kaminek M (2005) J Chromatogr A 1075:159–166
- Peres LEP, Mercier H, Kerbaudy GB, Zaffari GR (1997) Braz J Plant Physiol 9:169–176

11. Roshier PH, Jones HG, Hedden P (1985) *Planta* 165:91–99
12. Wang L, Bai J, Huang P, Wang HJ, Zhang LY, Zhao YQ (2006) *Electrochem Commun* 8(6):1035–1040
13. Zhong X, Yuan R, Chai YQ, Liu Y, Dai JY, Tang DP (2005) *Sens Actuators B* 104:191–198
14. Bonroy K, Friedt JM, Frederix F, Laureyn W, Langerock S, Campitelli A, Sara M, Borghs G, Goddeeris B, Declerck P (2004) *Anal Chem* 76:4299–4306
15. Wang RZ, Xiao LT, Yang MH, Ding JH, Qu FL, Shen GL (2006) *Chin Chem Lett* 17(12):1585–1588
16. Li J, Xiao LT, Zeng GM (2003) *Anal Chim Acta* 494:177–185
17. Wang J, Carmon KS, Luck LA, Suni II (2005) *Electrochem Solid-State Lett* 8(8):H61–H64
18. Li J, Xiao LT, Zeng GM, Huang GH, Shen GL, Yu RQ (2003) *Anal Chim Acta* 494:177–185
19. Long YT, Li CZ, Kraatz HB, Lee JS (2003) *Biophys J* 84:3218–3225
20. Rickert J, Göpel W (1996) *Biosens Bioelectron* 11(8):757–768
21. Xie Z, Zheng ZF, Chen FY (1996) *Acta Phytophysiol Sin* 22(3):284–290